The distribution of the ratio of consecutive level spacings in random matrix ensembles

Y. Y. Atas, E. Bogomolny, O. Giraud, and G. Roux

Univ. Paris-Sud, CNRS, LPTMS, UMR8626, 91405 Orsay, France.

(Dated: December 27, 2012)

We derive expressions for the probability distribution of the ratio of two consecutive level spacings for the classical ensembles of random matrices. This ratio distribution was recently introduced to study spectral properties of many-body problems, as, contrary to the standard level spacing distributions, it does not depend on the local density of states. Our Wigner-like surmises are shown to be very accurate when compared to numerics and exact calculations in the large matrix size limit. Quantitative improvements are found through a polynomial expansion. Examples from a quantum many-body lattice model and from zeros of the Riemann zeta function are presented.

Random matrix theory (RMT) was introduced half a century ago in order to describe statistical properties of energy levels of complex atomic nuclei [1]. Since then, it has proven to be very useful in a great variety of different fields [2, 3].

In quantum chaos [4], RMT accurately accounts for the spectral statistics of systems whose classical counterpart is chaotic. While for quantum Hamiltonians which classical counterpart is integrable, the Berry-Tabor conjecture [5] states that their level statistics follows a Poisson law, Bohigas, Giannoni and Schmit conjectured [6] that the case of quantum Hamiltonians with chaotic classical dynamics must fall into one of the three classical ensembles of RMT. These three ensembles correspond to Hermitian random matrices whose entries are independently distributed respectively real (GOE), complex (GUE) or quaternionic (GSE) random variables (see [2] for details).

Universality of RMT means that random matrix ensembles describe energy levels of real systems at a statistical level, and only in a local energy window when the mean level density is set to unity. Different models may and do have very different level densities and to compare usual spectral correlation functions like the nearest-neighbor spacing distribution one has to perform a transformation called unfolding [1, 2]. The unfolding procedure consists in changing variables from the true levels, e_n, to new ones, $\overline{e}_n = \overline{\mathcal{N}}(e_n)$, where $\overline{\mathcal{N}}(e)$ is the mean number of levels less than e, obtained either by smoothing over many realizations in the case of disordered systems, or by local smoothing over an energy window large compared to the level spacing but small compared to variations of $\overline{\mathcal{N}}(e)$. The unfolded spectrum has automatically a mean level spacing equal to one, and its statistical properties can thus be directly compared with those of RMT. When a functional form of $\overline{\mathcal{N}}$ is known (as for billiards), or when large enough statistics is available, the unfolding is straightforward and easily implemented.

The situation is different for many-body problems, where $\overline{\mathcal{N}}(e)$ increases as a stretched exponential function of energy [7] with, in general, unknown lower-order terms, and where it is difficult to calculate a large number of realizations because of an exponential increase of the Hilbert space dimension with the number of particles. In order to circumvent these difficulties which greatly diminish the precision of statistical tests in systems with a large number of particles, Oganesyan and Huse [8] proposed a new quantity defined as follows. Let e_n be an ordered set of energy levels and $s_n = e_{n+1} - e_n$ the nearest-neighbor spacings. Oganesyan and Huse considered the distribution of the ratios $\tilde{r}_n$ defined by

$$\tilde{r}_n = \frac{\min(s_n, s_{n-1})}{\max(s_n, s_{n-1})} = \min\left(r_n, \frac{1}{r_n}\right) , \qquad (1)$$

where

$$r_n = \frac{s_n}{s_{n-1}} . \qquad (2)$$

This quantity has the advantage that it requires no unfolding since ratios of consecutive level spacings are independent of the local density of states. Such a distribution thus allows a more transparent comparison with experiments than the traditional level spacing distribution. For this reason, many recent works use this quantity in different contexts of many-body systems. As an example let us mention quantum quenches, where the tools of RMT and quantum chaos were used as a phenomenological approach to quantify the distance from integrability on finite size lattices [9–11], and also to investigate numerically many-body localization [8, 12]. In these papers the distribution of consecutive level spacing ratios $P(\tilde{r})$ was shown to yield more precise results than the usual spacing distribution $P(s)$.

Although the distribution $P(r)$ plays a more and more important role in the interpretation of numerical data in quantum many-body Hamiltonians, only numerical estimates of it exist, and they are restricted to the GOE ensemble. RMT predictions for $P(r)$ are lacking. Such predictions are essential, both for understanding its shape for the three RMT ensembles, and for providing accurate estimates with simple formulas that could be used as an efficient tool.

This letter fills this gap by providing several important results on $P(r)$. First, we compute Wigner-like surmises for all three classical RMT ensembles, which already provide simple analytical formulae in very good agreement with exact numerics and analytical expressions in the large matrix size limit. Second, the remaining small differences are shown to

be well fitted to numerical precision by a rather simple polynomial expansion. Results are then applied to examples on a quantum many-body Hamiltonian and to zeros of the Riemann zeta function.

The ratio of consecutive level spacings distribution – Instead of the quantity (1), we find it more natural to consider directly the ratio of two consecutive level spacings (2) and its probability distribution $P(r)$. Indeed, let $\rho(e_1, e_2, e_3)$ be the probability density of three consecutive levels with $e_1 \leq e_2 \leq e_3$. Assuming translation invariance, $\rho(e_1, e_2, e_3) = P(s_1, s_2)$ where $s_i = e_{i+1} - e_i$. Then

$$P(r) \equiv \int P(s_1, s_2) \delta \left(r - \frac{s_1}{s_2} \right) \mathrm{d}s_1 \mathrm{d}s_2$$
$$= \int_0^\infty P(rs_2, s_2) s_2 \mathrm{d}s_2 . \tag{3}$$

It is physically natural and can be proved analytically that for all classical RMT ensembles in the bulk of the spectrum (as well as for Poisson variables) the function $P(s_1, s_2)$ is symmetric, that is, $P(s_1, s_2) = P(s_2, s_1)$. This left-right symmetry implies then that the distributions of r_n and $1/r_n$ are the same, so that $P(r)$ satisfies the following functional equation

$$P(r) = \frac{1}{r^2} P \left(\frac{1}{r} \right) . \tag{4}$$

Whenever (4) holds, it is equivalent to consider the whole distribution $P(r)$ or to restrict the study to the support $[0, 1]$ by considering the variable $\tilde{r}$ defined in (1), as was done in [8]. Here we concentrate on the whole distribution $P(r)$; since $P(\tilde{r}) = 2P(r)\Theta(1 - r)$, our results can easily be translated to the restricted distribution. The integrable (Poisson) case trivially yields $P(r) = 1/(1 + r)^2$. We now address the behavior of $P(r)$ for RMT ensembles.

Wigner-like surmise – For Gaussian ensembles, the joint probability distribution of N eigenvalues e_i is given by [2]

$$\rho(e_1, \dots, e_N) = C_{\beta, N} \prod_{1 \leq i < j \leq N} |e_i - e_j|^\beta \prod_{i=1}^N e^{-\beta e_i^2 / 2}, \tag{5}$$

where $C_{\beta, N}$ is a known normalization constant and β is the Dyson index equal to 1 (GOE), 2 (GUE) or 4 (GSE). The exact calculation of $P(r)$ via Eq. (3) requires the calculation of $P(s_1, s_2)$. Though this calculation is possible from (5) (as shown at the end of this Letter), it ultimately requires the use of numerical methods and is not transparent. Exactly the same problem appears in the calculation of the usual nearest-neighbor spacing distribution, $P(s)$, which is the probability that the distance between two consecutive levels is s. Rather than cumbersome exact calculations, Wigner derived a simple approximate expression for $P(s)$,

$$P_W(s) = a_\beta s^\beta e^{-b_\beta s^2} , \tag{6}$$

with some explicitly known normalization constants a_β and b_β [2]. This formula, called the Wigner surmise, corresponds

to the exact result for 2×2 matrices, and is in very good agreement with the exact large-N expressions [13].

In a similar spirit, we obtain a formula for the ratio distribution of two consecutive spacings by performing the exact calculation for 3×3 matrices, starting from the joint distribution (5) for three eigenvalues e_1, e_2, e_3. If for instance $e_1 \leq e_2 \leq e_3$, the ratio r is given by $(e_3 - e_2)/(e_2 - e_1)$. Consequently, the distribution $P(r)$ in the 3×3 case is proportional to

$$\int_{-\infty}^\infty de_2 \int_{-\infty}^{e_2} de_1 \int_{e_2}^\infty de_3 \, \rho(e_1, e_2, e_3) \, \delta \left(r - \frac{e_3 - e_2}{e_2 - e_1} \right) .$$

After the change of variables $x = e_2 - e_1, y = e_3 - e_2$, the integration over e_2 is trivial and the remaining integrals read

$$\iint_0^\infty dx dy \, \delta(rx - y) x^{\beta+1} y^\beta (x + y)^\beta e^{-\frac{1}{2}(x^2 + y^2) + \frac{1}{6}(x - y)^2} .$$

After performing the integrals, the surmise takes the simple form

$$P_W(r) = \frac{1}{Z_\beta} \frac{(r + r^2)^\beta}{(1 + r + r^2)^{1 + \frac{3}{2}\beta}}, \tag{7}$$

with Z_β the normalization constant (see values in Table I).

One can check that this result satisfies the symmetry (4). The distribution $P_W(r)$ has the same level repulsion at small r than $P(s)$, namely $P_W(r) \sim r^\beta$, while for large r the asymptotic behavior is $P_W(r) \sim r^{-(2+\beta)}$, contrary to the fast exponential decay of $P(s)$. This surmise also yields an analytic expression for the mean-values $\langle r \rangle_W$ and $\langle \tilde{r} \rangle_W$ widely used in the literature as a measure of chaoticity (see Table I for the exact values).

Comparison with numerics and polynomial fit – We now investigate the accuracy of the surmise (7) with respect to numerical calculations for large matrix sizes. As illustrated in Fig. 1, the surmise is almost indistinguishable from numerics and can thus be used for practical purposes as a reference to discriminate between regular and chaotic dynamics. The absolute difference $\delta P(r) = P_{\text{num}}(r) - P_W(r)$ between numerics and the surmise (7) is plotted in Fig. 2 for the three

Ens.	Poisson	GOE	GUE	GSE
Z_β	-	$\frac{8}{27}$	$\frac{4}{81}\frac{\pi}{\sqrt{3}}$	$\frac{4}{729}\frac{\pi}{\sqrt{3}}$
c_β	-	$2\frac{\pi-2}{4-\pi}$	$4\frac{4-\pi}{3\pi-8}$	$8\frac{32-9\pi}{45\pi-128}$
C	-	0.233378	0.578846	3.60123
$\langle r \rangle_W$	∞	$\frac{7}{4}$ $= 1.75$	$\frac{27}{8}\frac{\sqrt{3}}{\pi} - \frac{1}{2}$ ≈ 1.360735	$\frac{243}{80}\frac{\sqrt{3}}{\pi} - \frac{1}{2}$ ≈ 1.174661
$\langle r \rangle_{\text{fit}}$	-	1.7781(1)	1.3684(1)	1.1769(1)
$\langle \tilde{r} \rangle_W$	$2\ln 2 - 1$ ≈ 0.38629	$4 - 2\sqrt{3}$ ≈ 0.53590	$2\frac{\sqrt{3}}{\pi} - \frac{1}{2}$ ≈ 0.60266	$\frac{32}{15}\frac{\sqrt{3}}{\pi} - \frac{1}{2}$ ≈ 0.67617
$\langle \tilde{r} \rangle_{\text{fit}}$	-	0.5307(1)	0.5996(1)	0.6744(1)

TABLE I. Values of useful constants and averages $\langle r \rangle$ and $\langle \tilde{r} \rangle$. Averages $\langle . \rangle_W$ are calculated from Eq. (7), and $\langle . \rangle_{\text{fit}}$ from data in Fig. 1.
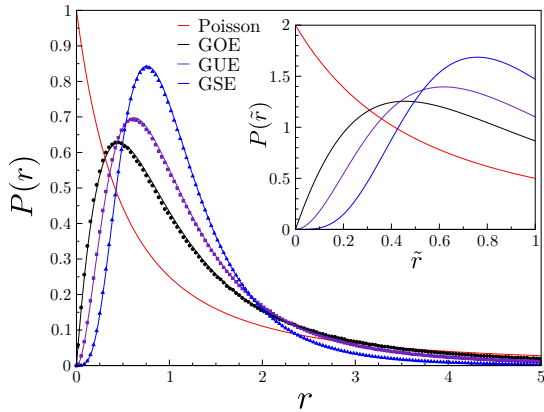
FIG. 1. (Color online) Distribution of the ratio of consecutive level spacings $P(r)$ for Poisson and RMT ensembles: full lines are the surmise Eq. (7), points are numerical results obtained by diagonalizing matrices of size $N = 1000$ with Gaussian distributed entries, averaged over 10^5 histograms. Inset: the distribution $P(\tilde{r})$.
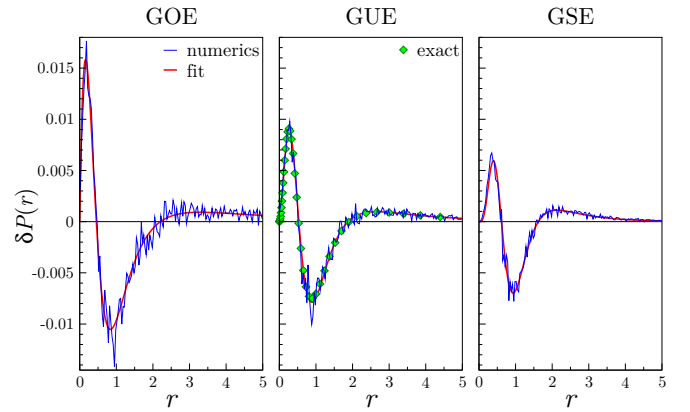

FIG. 2. (Color online) Difference $\delta P(r) = P_{\text{num}}(r) - P_W(r)$ between the numerics and the surmise (7). The fit function is given by Eq. (8). Green diamonds are results of exact calculations obtained from (9) for GUE.

ensembles, and has a maximum relative deviation of about 5%, similar to the Wigner surmise for $P(s)$ [13].

In order to go beyond the surmise (7), we propose a simple expression which perfectly fits this remaining difference $\delta P(r)$ within our computational accuracy. In order to fulfill Eq. (4), and assuming that $P(r)$ for large N and $P_W(r)$ have the same asymptotic behavior for small and large r, a reasonable ansatz is the following expansion

$$\delta P_{\text{fit}}(r) = \frac{C}{(1+r)^2}\left[\left(r + \frac{1}{r}\right)^{-\beta} - c_\beta\left(r + \frac{1}{r}\right)^{-(\beta+1)}\right],$$
(8)

where c_β is easily calculated from the normalization condition $\int_0^\infty \delta P(r) dr = 0$ (see Table I for the exact value). Thus the large-N expression for $P(r)$ can be fitted by the expression $P(r) = P_W(r) + \delta P_{\text{fit}}(r)$ with only one fitting parameter, which is the overall magnitude C of the discrepancy. The best fit C can be found in Table I. The corresponding curves are shown in Fig. 2. Thanks to these very good fits, one can quickly infer accurate predictions for $\langle r \rangle$ and $\langle \tilde{r} \rangle$ and any average weighted by $P(r)$ (see Table I).

Large-N calculation – We now turn to the exact calculation of $P(r)$ for GUE (i.e. $\beta = 2$) in the limit $N \to \infty$, following a path similar to the derivation of the exact level spacing distribution $P(s)$.

Our starting point is Eq. 5.4.29 of Ref. 2. From that equation, one can check that the probability $p(-t, y, t)$ of having three consecutive levels at points $-t, y, t$ can be rewritten as

$$p(-t, y, t) = \det(1 - K)\det[R(x, z)_{x, z = -t, y, t}], \quad (9)$$

where $R(x, y)$ is the resolvent kernel, i. e. the kernel of the operator $(1 - K)^{-1}K$, and $\det(1 - K)$ is the Fredholm determinant of K. Operator K is an integral operator whose action

is defined as

$$(Kf)(x) = \int_{-t}^{t} K(x, y)f(y)\mathrm{d}y \quad (10)$$

with the kernel

$$K(x, y) = \frac{\sin \pi(x - y)}{\pi(x - y)} . \quad (11)$$

It is known (see e. g. [14]) that for a kernel of this form the resolvent kernel can be written as

$$R(x, y) = \frac{Q(x)P(y) - Q(y)P(x)}{x - y}, \quad (12)$$

with functions $Q(x)$ and $P(x)$ obeying integral equations

$$Q(x) - \int_{-t}^{t} K(x, y)Q(y)\mathrm{d}y = \frac{\sin \pi x}{\pi},$$

$$P(x) - \int_{-t}^{t} K(x, y)P(y)\mathrm{d}y = \cos \pi x. \quad (13)$$

Function $Q(x)$ and $P(x)$ have many useful properties which allow to relate the calculation of spectral statistics for standard RMT ensembles to solutions of Painlevé equations (see e. g. [14] and references therein). Though this approach is elegant, it still requires numerical resolution of Painlevé V equation for $\det(1 - K)$ with subsequent solutions of linear equations for $Q(x)$ and $P(x)$ whose coefficients are determined by that solution.

We find it simpler to use the direct method proposed in [15] for computing $\det(1 - K)$. It is based on a quadrature method for numerical evaluation of the integrals

$$\int_{-t}^{t} f(x)dx = \sum_{k=1}^{m} w_k f(x_k) \quad (14)$$

appearing in the definition (10) of the integral operator K. Such a discretization allows to approximate the determinant
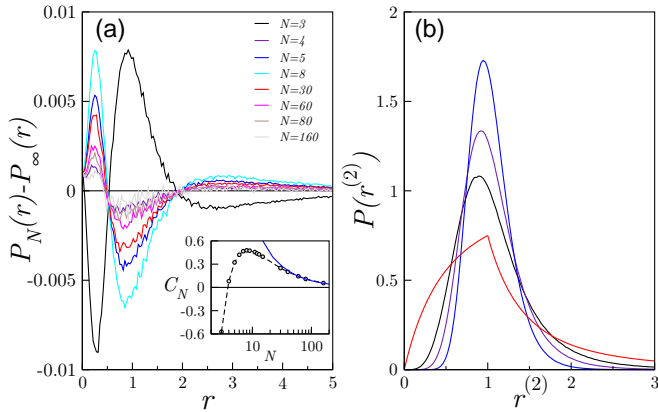
FIG. 3. (Color online) (a) $P(r) - P_\infty(r)$ for GUE and various matrix sizes. Inset: constant C_N from the fit (8) as a function of matrix size N (solid line is a fit $1/N$). (b) Density distributions for the overlapping ratio $r_n^{(2)} = (e_{n+2} - e_n)/(e_{n+1} - e_{n-1})$ for Poisson variables and for the three classical RMT ensembles (same color code as in Fig. 1).
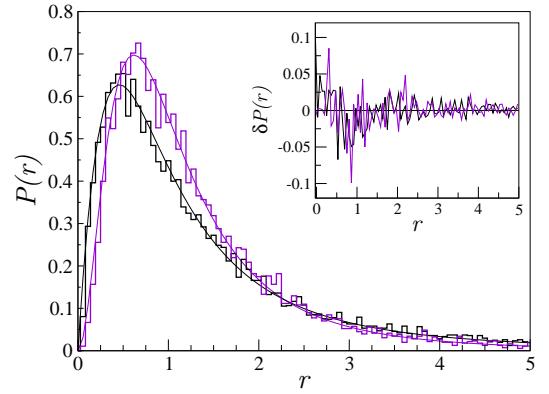

FIG. 4. (Color online) Histogram of the ratio of consecutive level spacings $P(r)$. Black: Quantum Ising model in fields $\lambda = \alpha = 0.5$ in sector of eigenvectors of $\hat{T}$ with eigenvalue ω_3 ($\omega_j = \exp(2i\pi j/L)$, $j = 0, 1, \ldots, L-1$), for $L = 18$ spins (dimension of eigenspace = 14541). Violet: The same for zeros of Riemann zeta function up the critical line (10^4 levels starting from the 10^{22}th zero, taken from [18]). Full lines correspond to the Wigner-like surmise Eq. (7) with respectively $\beta = 1$ and $\beta = 2$. Inset: Difference between the numerics and these surmises.

of the integral operator as a finite $m \times m$ determinant

$$\det(1 - K) \approx \det\left(\delta_{jk} - K(x_j, x_k)w_k\right) \qquad (15)$$

and functions $Q(x)$ and $P(x)$ defined in (13) can be obtained by solving a linear system of m equations. As noted in [15] the method quickly converges. The result is presented in Fig. 2, where the Clenshaw-Curtis method with up to 60 points of discretization has been used for the discretization (14). Figure 3 (left) shows how the numerical results converge to the analytic large-N calculation. As mentioned previously, the fit $P(r) = P_W(r) + \delta P_{\text{fit}}(r)$ works well for all N, with an overall N-dependent constant C_N in (8). This constant, which gives the amplitude of the departure from the Wigner-like surmise, asymptotically decreases as $1/N$ (see inset of Fig. 3).

Applications – To illustrate the above formalism, we investigate the spectral properties of a quantum Ising chain of L spins$-\frac{1}{2}$ with periodic boundary conditions in transverse field λ and longitudinal field α. The Hamiltonian is given by

$$\hat{H} = -\sum_{n=1}^{L} \left(\hat{\sigma}_n^x \hat{\sigma}_{n+1}^x + \lambda \hat{\sigma}_n^z + \alpha \hat{\sigma}_n^x\right), \qquad \hat{\sigma}_{L+1}^x = \hat{\sigma}_1^x \tag{16}$$

where $\hat{\sigma}_n^{x,z}$ are the Pauli matrices at site n. This model recently attracted attention due to its experimental realization in cobalt niobate ferromagnet [16]. The Hamiltonian (16) commutes with the operator $\hat{T}$ which translates the state by one lattice spacing and obeys $\hat{T}^L = 1$. Consequently, $\hat{H}$ takes a block diagonal form in the basis of eigenstates of $\hat{T}$, and one has to consider separately each sector of symmetry. The result for one sector is illustrated in Fig. 4. Other symmetry sectors give similar results. As expected, $P(r)$ agrees well with the GOE prediction (7) with $\beta = 1$.

Another example of application is to look at non-trivial ze-

ros of the Riemann zeta function

$$\zeta(s) = \sum_{n=1}^{\infty} \frac{1}{n^s}. \tag{17}$$

It is well established that statistical properties of Riemann zeros are well described by the GUE distribution [17]. The probability distribution of the ratio of two consecutive spacings of these zeros, presented in Fig. 4, is in a perfect agreement with GUE formula (7) with $\beta = 2$.

Conclusion – The investigation of spectral statistics in many-body problems with a large number of particles attracted wide attention in recent years. The absence of a well established expression for the mean density of states greatly diminishes the usefulness of standard correlation functions such as the nearest-neighbor spacing distribution. To avoid this problem, a new statistical tool has been proposed in [8], namely the distribution of the ratio of two consecutive level spacings.

The main result of the paper is the derivation of simple approximative formulae for this distribution for classical RMT ensembles. The resulting Wigner-like surmises agree very well with direct numerical calculations. The difference between the surmise and the exact calculations is small and can be fitted by a one-parameter polynomial formula with excellent accuracy.

In the same spirit, several different ratios can be introduced which generalize the quantity (2). Analytic expressions and Wigner-like surmises can be derived in a similar way for the density distributions of these quantities, and will be discussed elsewhere. An example is given in Fig. (3) (right). All these distributions are universal in the sense that they apply without any unfolding or renormalization to spectra ranging from many-body systems to Riemann zeta function.

---

[1] C. E. Porter, *Statistical Theories of Spectra: Fluctuations* (Academic Press, New York), 1965;

[2] M. L. Mehta, *Random Matrix Theory*, Springer, New York (1990).

[3] G. Akemann, J. Baik, and P. Di Francesco, *The Oxford Handbook of Random Matrix Theory* (Oxford University Press, 2011).

[4] T. A. Brody et al., Rev. Mod. **53**, 385 (1981); T. Guhr, A. Müller-Groeling, H. A. Weidenmüller, Phys. Rep. **299**, 189 (1998).

[5] M. Berry and M. Tabor, Proc. R. Soc. Lond A **356**, 375 (1977).

[6] O. Bohigas, M.-J. Giannoni, and C. Schmit, Phys. Rev. Lett. **52**, 1 (1984).

[7] H. A. Bethe, Phys. Rev. **50**, 332 (1936).

[8] V. Oganesyan and D. A. Huse, Phys. Rev. B **75**, 155111 (2007).

[9] C. Kollath, G. Roux, G. Biroli, and A. M. Läuchli, J. Stat. Mech. (2010) P08011.

[10] M. Rigol and L. F. Santos, Phys. Rev. A **82**, 011604(R) (2010); L. F. Santos and M. Rigol, Phys. Rev. E **82**, 031130 (2010); Phys. Rev. E **81**, 036206 (2010).

[11] M. Collura, H. Aufderheide, G. Roux, and D. Karevski, Phys. Rev. A **86**, 013615 (2012).

[12] V. Oganesyan, A. Pal, and D. A. Huse, Phys. Rev. B **80**, 115104 (2009); A. Pal and D. A. Huse, Phys. Rev. B **82**, 174411 (2010); E. Cuevas, M. Feigel'man, L. Ioffe, and M. Mézard, Nature Comm. **3**, 1128 (2012); G. Biroli, A. C. Ribeiro-Teixeira, M. Tarzia, arXiv:1211.7334 (2012); S. Iyer, V. Oganesyan, G. Refael, and D. A. Huse, arXiv:1212.4159 (2012).

[13] B. Dietz and F. Haake, Z. Phys. B – Condensed Matter **80**, 153 (1990).

[14] C. A. Tracy and H. Widom, *Introduction to random matrices*, in Geometric and quantum aspects of integrable systems (1993) 103.

[15] F. Bornemann, Math. Comput. **79**, 871 (2010).

[16] R. Coldea et al., Science **8**, **327**, 177 (2010).

[17] H. L. Montgomery, Proc. Symp. Pure Math. **24**, 181 (1973); E. B. Bogomolny and J. P. Keating, Nonlinearity **8**, 1115 (1995); *ibid* Nonlinearity **9**, 911 (1995); Z. Rudnick and P. Sarnak, Duke Math. J. **81**, 269 (1996); J. P. Keating and N. C. Snaith, Comm. Math. Phys. **214**, 57 (2000).

[18] A. Odlyzko, web page: www.dtc.umn.edu/~odlyzko/.